Che-1 phosphorylation by ATM/ATR and Chk2 kinases activates p53 transcription and the G_2/M checkpoint

Tiziana Bruno,[1,11] Francesca De Nicola,[2,3,11] Simona Iezzi,[2,3] Daniele Lecis,[4] Carmen D'Angelo,[1] Monica Di Padova,[2,3] Nicoletta Corbi,[5] Leopoldo Dimiziani,[6] Laura Zannini,[4] Christian Jekimovs,[7] Marco Scarsella,[1] Alessandro Porrello,[8] Alberto Chersi,[9] Marco Crescenzi,[6] Carlo Leonetti,[1] Kum Kum Khanna,[7] Silvia Soddu,[8] Aristide Floridi,[2,3] Claudio Passananti,[3,5,10] Domenico Delia,[4] and Maurizio Fanciulli[3,10,*]

[1] Experimental Chemotherapy Laboratory, Department of Experimental Oncology, Regina Elena Cancer Institute, 00158 Rome, Italy
[2] Department of Experimental Medicine, University of L'Aquila, 67100 L'Aquila, Italy
[3] Laboratory B, Department of Therapeutic Programs Development, Regina Elena Cancer Institute, 00158 Rome, Italy
[4] Department of Experimental Oncology, Istituto Nazionale Tumori, 20133 Milan, Italy
[5] Istituto di Biologia e Patologia Molecolare, CNR, 00158 Rome, Italy
[6] Department of Environment and Primary Prevention, High Institute of Health, 00161 Rome, Italy
[7] Queensland Institute of Medical Research, P.O. Royal Brisbane Hospital, Brisbane, Queensland 4029, Australia
[8] Molecular Oncogenesis Laboratory, Department of Experimental Oncology, Regina Elena Cancer Institute, 00158 Rome, Italy
[9] Laboratory D, Department of Therapeutic Programs Development, Regina Elena Cancer Institute, 00158 Rome, Italy
[10] Rome Oncogenomic Center, Regina Elena Cancer Institute, 00158 Rome, Italy
[11] These authors contributed equally to this work.
*Correspondence: fanciulli@ifo.it

Summary

Che-1 is a RNA polymerase II-binding protein involved in the transcription of E2F target genes and induction of cell proliferation. Here we show that Che-1 contributes to DNA damage response and that its depletion sensitizes cells to anticancer agents. The checkpoint kinases ATM/ATR and Chk2 interact with Che-1 and promote its phosphorylation and accumulation in response to DNA damage. These Che-1 modifications induce a specific recruitment of Che-1 on the *TP53* and *p21* promoters. Interestingly, it has a profound effect on the basal expression of p53, which is preserved following DNA damage. Notably, Che-1 contributes to the maintenance of the G_2/M checkpoint induced by DNA damage. These findings identify a mechanism by which checkpoint kinases regulate responses to DNA damage.

Introduction

In DNA damage response (DDR), eukaryotic cells activate checkpoint pathways to arrest the cell cycle and facilitate DNA repair or induce apoptosis (Hoeijmakers, 2001; Bartek and Lukas, 2001; Zhou and Elledge, 2000). Ataxia-telangiectasia mutated (ATM) and checkpoint kinases Chk1 and Chk2 are early and key mediators of DDR through activation of an increasing number of substrates (Shiloh, 2003; Kastan and Lim, 2000; Bartek and Lukas, 2003) such as p53, NBS1, BRCA1, MDM2, Cdc25A, Cdc25C, and E2F1 (Shiloh, 2003; Kastan and Lim, 2000; Bartek and Lukas, 2003). The relevance of these kinases in the maintenance of genome integrity is clearly indicated by the severe human genetic disorders and the predisposition to cancer associated with defects in these proteins (Hoeijmakers, 2001; van Gent et al., 2001; Khanna and Jackson, 2001). In addition, DDR was identified as a potent anticancer barrier in human precancerous lesions (Bartkova et al., 2005; Gorgoulis et al., 2005).

p53 is a tumor suppressor mainly involved in the transcriptional regulation of a large number of growth-arrest- and apoptosis-related genes (Levine, 1997; el-Deiry et al., 1992). Upon genotoxic damage, p53 contributes to cell-cycle arrest at the G_1/S and/or G_2/M checkpoints through diverse mechanisms (Wahl and Carr, 2001). To exert these functions, p53 that is constitutively expressed at very low levels and in an inactive conformation must be induced and activated (Ryan et al., 2001; Prives and Hall, 1999). These events are thought to depend mainly on posttranslational modifications that include phosphorylation by

SIGNIFICANCE

The DNA-damage-signaling pathway is a highly conserved response to genotoxic stresses. In this pathway, ATM/ATR are generally sensors of DNA damage, but, together with the checkpoint kinases Chk1 and Chk2, they also function as response effectors by phosphorylation of key substrates, such as p53, BRCA1, and NBS1. In particular, p53 phosphorylation leads to protein accumulation and activation, which in turn promotes cell-cycle arrest or apoptosis. Here we describe a mechanism by which ATM/ATR and Chk2 can regulate p53 expression through Che-1 phosphorylation and stabilization. Essentially, Che-1 inhibition potentiates the cytotoxicity of anticancer drugs, thus suggesting Che-1 as a possible therapeutic target to increase the efficacy of DNA-damaging drugs.

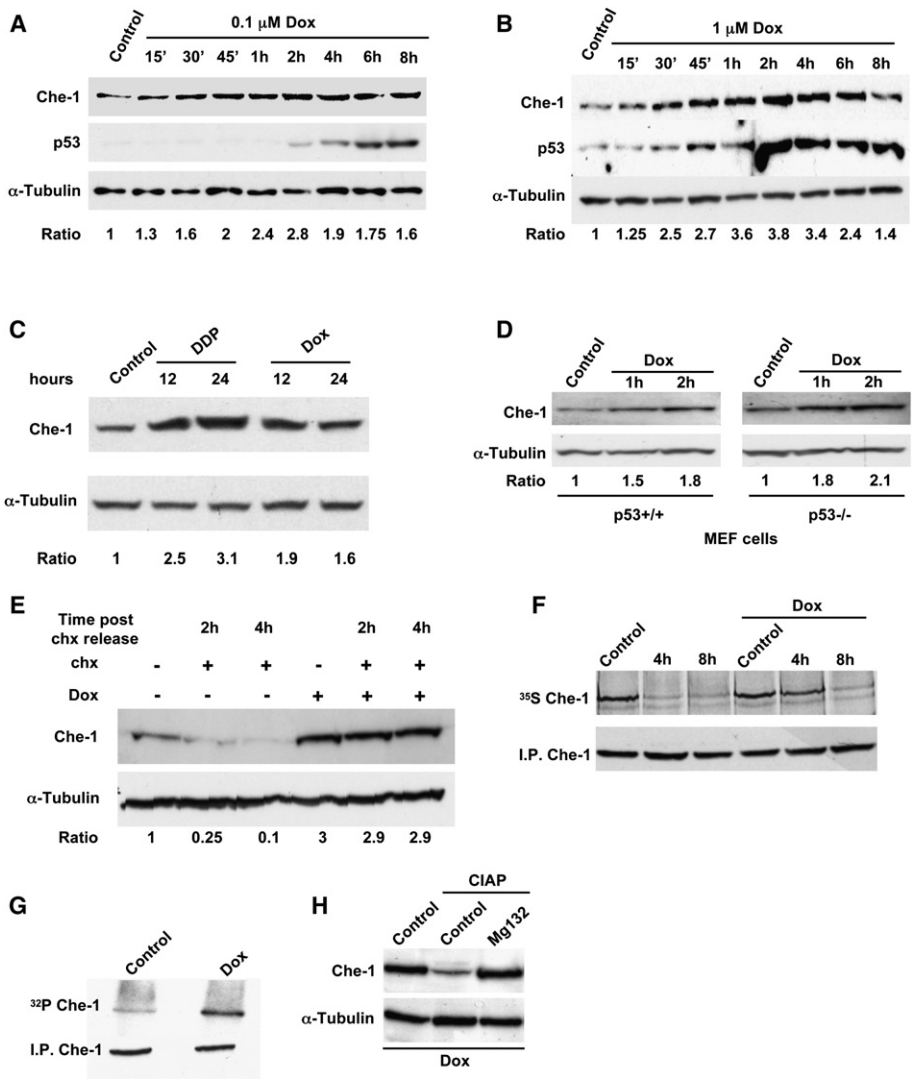

Figure 1. DNA damage induces Che-1 protein stabilization

A and B: WB of TCEs from HCT116 cells exposed to 0.1 (**A**) or 1 μM (**B**) Dox.

C: WB analysis with the indicated Abs of HCT116 cells explanted from untreated or DDP- or Dox-treated (10 mg/kg) nude mice.

D: WB for the indicated protein of TCEs from $p53^{+/+}$ or $p53^{-/-}$ MEFs treated with 1 μM Dox for the indicated times.

E: WB of TCEs from HCT116 cells incubated with or without 1 μM Dox for 2 hr. 20 μM chx was then added for the indicated times.

F: Top: HCT116 cells treated with or without 1 μM Dox for 1 hr were incubated with ^{35}S methionine for 20 min. TCEs were collected at the indicated times and immunoprecipitated with anti-Che-1 Ab. Bottom: the same gel blotted and incubated with anti-Che-1 Ab.

G: Top: autoradiography of immunoprecipitates with anti-Che-1 Ab from HCT116 cells incubated with ^{32}P inorganic orthophosphate and treated with or without 1 μM Dox for 2 hr. Bottom: the same gel blotted and incubated with anti-Che-1 Ab.

H: HCT116 cells were incubated with 1 μM Dox with or without 10 μM MG132 for 2 hr. TCEs were incubated for 30 min with CIAP and immunoblotted with anti-Che-1 or anti-α-tubulin Abs.

ATM/ATR, Chk1, and Chk2 kinases, at least upon certain stress stimuli (Banin et al., 1998; Shieh et al., 2000; Hirao et al., 2000). However, increasing evidence supports a role for p53 regulation also at the transcription level (Sun et al., 1995; Hellin et al., 1998; Pei et al., 1999; Takaoka et al., 2003).

Human Che-1 is a highly conserved RNA polymerase II (Pol II)-binding protein that regulates gene transcription and cell proliferation (Fanciulli et al., 2000; Thomas et al., 2000; Lindfors et al., 2000; Page et al., 1999; Burgdorf et al., 2004; Bruno et al., 2002). Che-1 interacts with Rb and affects its growth suppression activity by interfering with the Rb-mediated recruitment of histone deacetylase I on the promoters of E2F1-responsive genes (Fanciulli et al., 2000; Bruno et al., 2002). Traube, the mouse homolog of Che-1, is essential for proliferation of preimplantation embryos (Thomas et al., 2000). Despite this proproliferative role of Che-1/Traube, we observed that Che-1 is downregulated in several tumors compared to matching normal tissues, with an incidence of 80% in the colon carcinomas examined (Di Padova et al., 2003). In agreement, Che-1 overexpression caused cell-cycle arrest in colon carcinoma cells by induction of the CDK inhibitor $p21^{Waf1}$ (p21) (Di Padova et al., 2003). The latter finding prompted us to investigate Che-1 regulation in DDR. Here, we show that DNA damage by different genotoxic agents is associated with Che-1 phosphorylation and extended half-life. These posttranslational modifications are induced by ATM and Chk2, which phosphorylate Che-1 on specific residues and are functionally linked to the DNA-damage-induced G_2/M checkpoint. Moreover, microarray and chromatin immunoprecipitation analyses show that Che-1 activates the transcription of p53 and consequently of several p53 target genes, suggesting a pathway by which ATM and Chk2 may modulate p53 levels. Finally, we show that Che-1 depletion strongly sensitizes tumor cells to anticancer drugs, suggesting Che-1 as a possible therapeutic target to increase the efficacy of antitumor agents.

Results

DNA damage stabilizes Che-1 protein

To investigate the involvement of Che-1 in DDR, HCT116 human colon carcinoma cells were treated with different genotoxic agents, including the anticancer drugs doxorubicin (Dox) and cisplatin (DDP), UV light, or ionizing radiations (IR). Early accumulation of Che-1 was detectable upon each treatment at both sublethal (0.1 μM Dox; Figure 1A) and lethal (1 μM Dox; Figure 1B) doses of agents, in a time- and dose-dependent manner (Figures 1A and 1B and Figures S1A, S1B, and S1C [see the

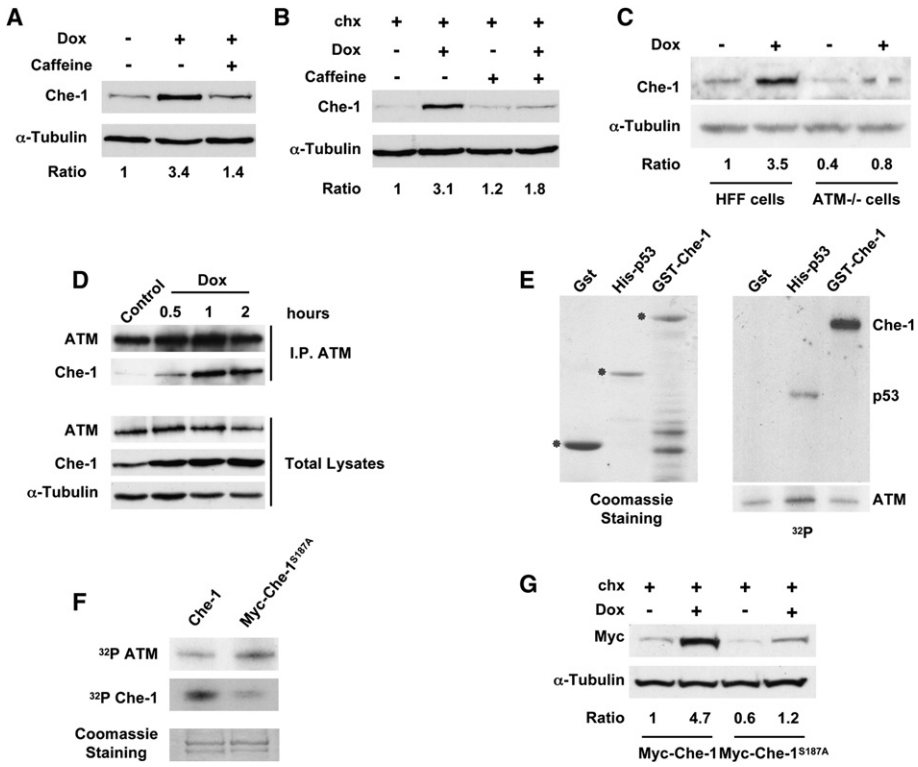

Figure 2. ATM/ATR regulates Che-1

A and B: WB of TCEs from HCT116 cells treated with the indicated drugs for 2 hr (1 μM Dox, 10 mM caffeine), and then with 20 μM chx for an extra 2 hr.

C: HFF and AT cells were treated with or without 1 μM Dox for 2 hr, and WB was performed with the indicated Abs.

D: TCEs from HCT116 cells treated for the indicated times with 1 μM Dox were immunoprecipitated with anti-ATM Ab and analyzed by WB with the indicated Abs.

E: Specific phosphorylation of Che-1 by ATM/ATR. Flag-ATM was immunoprecipitated from 293 transfected cells and employed in an in vitro reaction to phosphorylate GST, His-p53, and GST-Che-1 proteins. The left panel shows Coomassie blue staining of purified GST and 6×His fusion proteins (as indicated by asterisks); the right panel depicts the ^{32}P autoradiograph of the kinase assay performed with equal amounts of GST and 6×His fusion proteins.

F: In vitro phosphorylation of Che-1 at Ser187. GST-Che-1 or the GST-Che-1^{S187A} mutant was used as substrate for ATM kinase assay. The upper and middle panels depict ATM and Che-1 ^{32}P autoradiographs, and the lower panel shows Coomassie blue stain of purified GST-Che-1 proteins.

G: HCT116 cells were transfected with Myc-Che-1 or Myc-Che-1^{S187A} mutant. At 48 hr posttransfection, cells were treated as described in **A**, and TCEs were analyzed by WB with the indicated Abs.

Supplemental Data available with this article online]). In agreement, Che-1 accumulated in vivo in HCT116 cells injected in nude mice and treated with drugs (Figure 1C). In addition, Che-1 accumulation was detectable in primary mouse embryo fibroblasts (MEFs) (Figure 1D, left panel) and preceded the expected p53 upregulation in each tested condition (Figures 1A and 1B and data not shown). Thus, to assess whether Che-1 accumulation is independent of p53, MEFs from wild-type (WT) ($p53^{+/+}$) and KO ($p53^{-/-}$) mice were treated with Dox. Comparable induction of Che-1 was detected in the two populations (Figure 1D), indicating that Che-1 levels are increased in DDR independently of p53.

To identify the mechanism(s) of Che-1 accumulation, Dox-treated and untreated HCT116 cells were employed. No differences were observed in *Che-1* mRNA levels and *Che-1* promoter activity, as assessed by northern blotting and luciferase reporter assay, respectively (data not shown). In contrast, Dox treatment strongly increased the levels of transfected Myc-tagged Che-1 (Myc-Che-1), whose expression is driven by a heterologous promoter (data not shown), suggesting the presence of a posttranslational regulation. Thus, we tested the half-life of Che-1 in Dox-treated and untreated HCT116 cells either in the presence of the translation inhibitor cycloheximide (chx), or by pulse-chase of ^{35}S-methionine metabolic labeled cells. The half-life of Che-1 was strongly increased (from <2 hr to >4 hr) by Dox treatment (Figures 1E and 1F), indicating that DDR induces Che-1 accumulation by promoting its stability. In addition, cell treatment with the proteasome inhibitor MG132 increased the half-life of Che-1 to a similar extent as Dox-treatment (Figure S1D), suggesting the involvement of the proteasome system in the regulation of Che-1 stability. Taken together, these data show that DDR is associated with a p53-independent, posttranslational modification-driven stabilization of Che-1.

DNA-damage-induced phosphorylation of Che-1 counteracts its degradation

DDR is regulated, at the early steps, by a series of kinases that activate downstream targets, such as p53 and E2F1, through their phosphorylation and subsequent stabilization (Banin et al., 1998; Hirao et al., 2000). Thus, we evaluated whether Che-1 was phosphorylated in DDR. Che-1 was immunoprecipitated from ^{32}P-orthophosphate-labeled HCT116 treated or not with Dox. Upon normalization of the amount of the immunoprecipitated proteins (Figure 1G, lower panel), a strong increase of Che-1 phosphorylation was detected after Dox treatment (Figure 1G, upper panel), showing that Che-1 can be phosphorylated in vivo at least in this stressing condition.

To test whether Dox-induced phosphorylation of Che-1 is linked to its stabilization, total cell extracts (TCEs) were prepared from Dox-treated HCT116 cells in the presence of ATP and glycerol to preserve the integrity of the 26S proteasome (Canu et al., 2000). TCEs were subsequently incubated with calf intestinal alkaline phosphatase (CIAP) in the presence or absence of MG132 and analyzed by western blotting (WB). CIAP treatment substantially reduced Dox-induced stabilization of Che-1, but MG132 prevented this reduction (Figure 1H), suggesting that phosphorylation is involved in Che-1 stabilization.

Che-1 is an ATM substrate

ATM and ATR are ser/thr kinases that phosphorylate several critical checkpoint proteins in DDR (Shiloh, 2003; Kastan and Lim, 2000). Thus, we tested whether these kinases are involved in Che-1 accumulation by using the specific inhibitor caffeine (Sarkaria et al., 1999). Preincubation of cells with caffeine interfered with Dox-induced accumulation of Che-1 (Figure 2A). This effect was dependent on caffeine-mediated inhibition of Che-1 stabilization, as shown by the absence of Che-1 accumulation

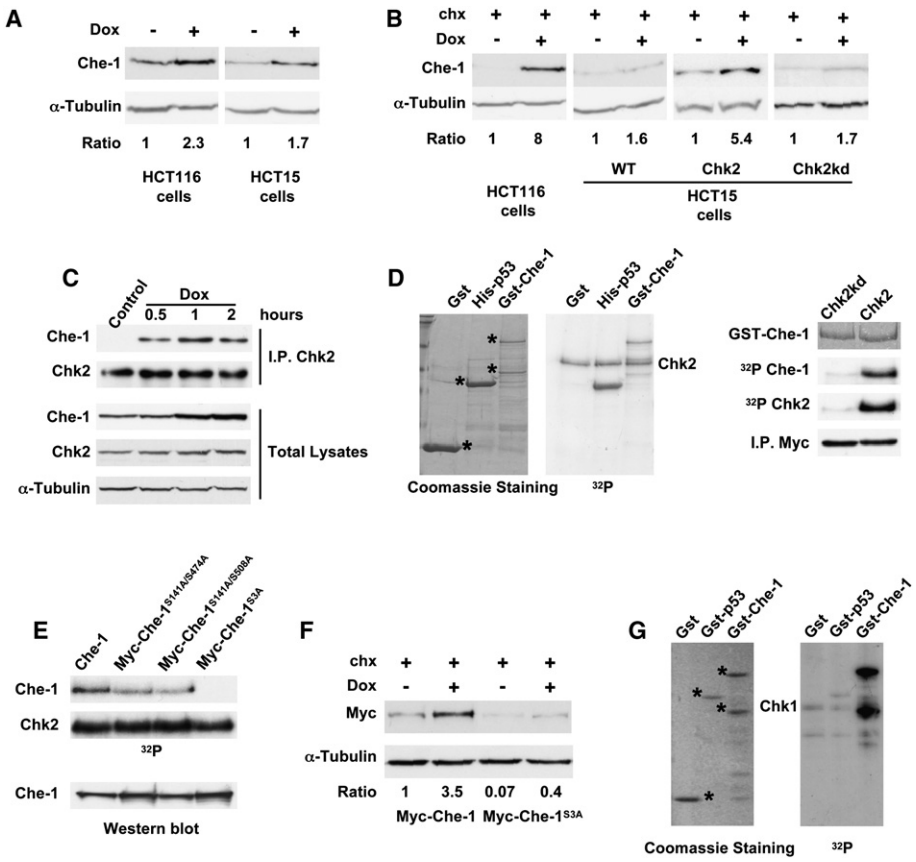

Figure 3. Chk2 phosphorylates Che-1

A: WB of HCT116 and HCT15 cells treated with or without 1 μM Dox.

B: HCT116 and HCT15 cells or HCT15 cells stably expressing either WT or kd Chk2 were treated with or without 1 μM Dox for 2 hr and then with 2 μM chx for an extra 2 hr. TCEs were analyzed as in **A**.

C: TCEs from HCT116 cells treated with 1 μM Dox for the indicated times were immunoprecipitated with anti-Chk2 Ab and analyzed by WB with the indicated Abs.

D: Specific phosphorylation of Che-1 by Chk2. Myc-Chk2 or Myc-Chk2 kd were immunoprecipitated from transfected 293 cells and employed in in vitro reactions to phosphorylate GST, His-p53, and GST-Che-1 proteins. The left panel shows Coomassie blue staining of purified recombinant proteins (as indicated by asterisks), the middle panel depicts the ^{32}P autoradiograph of the same gel, and the right panel shows an in vitro kinase assay performed with Chk2 and Chk2 kd.

E: GST-Che-1 recombinant proteins were used as substrates for a Chk2 kinase assay in vitro. The upper panel depicts Chk2 and Che-1 ^{32}P autoradiographs, and the lower panel shows the blot of the gel analyzed with anti-Che-1 Ab.

F: HCT116 cells were transfected with Myc-Che-1 or the Myc-Che-1^{S3A} mutant. At 48 hr posttransfection, cells were treated with Dox and chx as indicated, and WB was performed with the indicated Abs.

G: Specific phosphorylation of Che-1 by Chk1. Flag-Chk1 was immunoprecipitated from 293 transfected cells and used to phosphorylate GST, GST-p53, and GST-Che-1 proteins in in vitro reaction. The left panel shows Coomassie blue staining of purified recombinant proteins (as indicated by asterisks), and the right panel depicts the ^{32}P autoradiograph of the same gel.

upon Dox treatment in the presence of chx (Figure 2B). A direct role of ATM in Dox-induced stabilization of Che-1 was confirmed by its severe impairment in human fibroblasts from ataxia telangiectasia (AT) patients when matched up to normal human fetal fibroblasts (HFF) (Figure 2C). Comparable results were obtained by depleting ATM with small interfering RNA (siRNA) in HCT116 cells (Figure S2A), supporting a role for ATM in DNA-damage-induced Che-1 accumulation.

Next, using TCEs from HCT116 cells, we tested whether the endogenous ATM and Che-1 proteins can physically interact. Though low levels of Che-1 coprecipitated with ATM in control cells, increasing amounts of Che-1 were coprecipitated after Dox treatment (Figure 2D), indicating that the two proteins belong to a same complex and that Dox treatment increases the presence of Che-1 in this complex. We then examined whether ATM directly phosphorylates Che-1 by in vitro kinase assays. Recombinant GST-Che-1 was used as substrate for Flag-ATM immunoprecipitated from 293 cells. The presence of a specific phosphorylation signal on GST-Che-1 and His-p53 positive control, but not on GST alone (Figure 2E), indicated that Che-1 can be phosphorylated by ATM in vitro. Similar results were obtained by performing the kinase assay with ATR (Figure S2B), indicating that Che-1 can also be a target for this kinase. The absence of Che-1 phosphorylation by the kinase-dead forms of ATM and ATR demonstrated the specificity of these reactions (Figure S2B).

Three putative ATM/ATR consensus sites (Kim et al., 1999; O'Neill et al., 2000) are present in Che-1 at residues Ser187, Thr391, and Thr407. To identify the target(s), GST fusion polypeptides covering the whole Che-1 protein were used as substrates in in vitro kinase assays with Flag-ATM. Only the GST-164-270 polypeptide carrying Ser187 was phosphorylated by ATM (Figure S2C). In addition, substitution of Che-1 Ser187 with an alanine (Che-1^{S187A}) prevented Che-1 phosphorylation by ATM (Figure 2F), supporting this residue as an ATM-target site.

To evaluate whether this phosphorylation site plays a role in Che-1 stabilization, we compared the expression levels of exogenous Myc-Che-1 and Myc-Che-1^{S187A} proteins in HCT116 cells. The Dox-induced accumulation of Che-1 was strongly reduced, though not completely abolished, in the Myc-Che-1^{S187A} mutant (Figure 2G), indicating that Che-1 Ser187 is phosphorylated by ATM/ATR in DDR and that this phosphorylation contributes to increase Che-1 stability.

Che-1 is a Chk2 substrate

The residual stabilization capacity of the Myc-Che-1^{S187A} mutant suggests that other kinases might be involved in Che-1 stabilization. Since we previously identified Che-1 in a yeast two-hybrid screen using Chk2 as bait (D.L. and L.Z., unpublished data), we tested whether this kinase is also involved in Che-1 regulation. Dox-induced Che-1 accumulation and stabilization were assessed in Chk2-proficient HCT116 and Chk2-defective HCT15 cells (Bell et al., 1999). Although Che-1 levels increased in both cell lines, most likely due to Chk1 kinase operating in a redundant manner (Figure 3A), reduced Che-1 stabilization was observed in HCT15 cells (Figure 3B), which was rescued

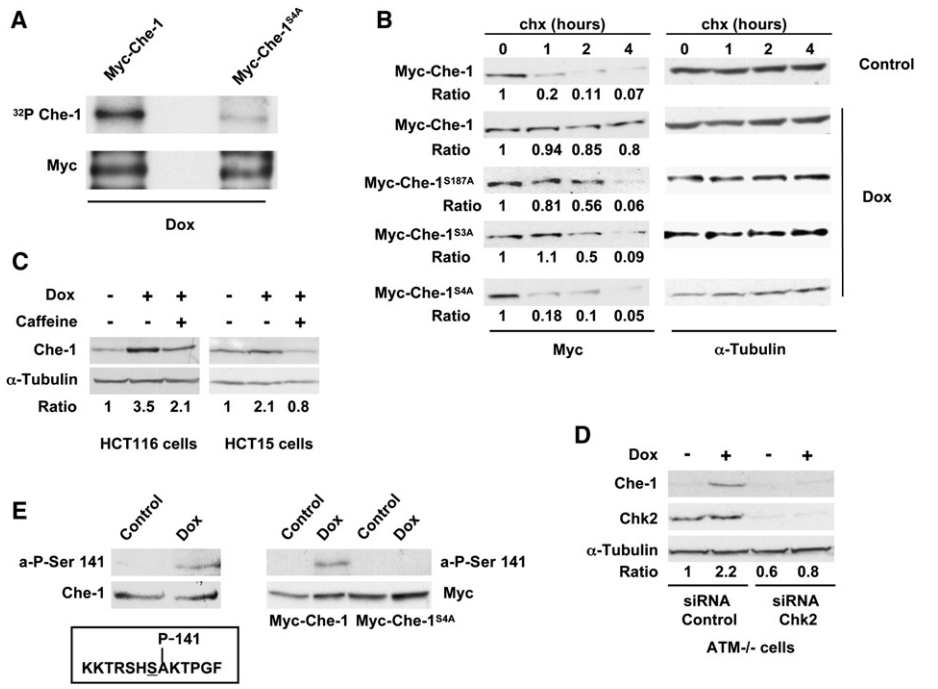

Figure 4. Che-1 is stabilized by ATM/ATR and Chk2 phosphorylation

A: Top: autoradiography of immunoprecipitates with anti-Myc Ab from HCT116 cells transfected with Myc-Che-1 or the Myc-Che-1^{S4A} mutant, incubated with ^{32}P ortophosphate, and treated with 1 μM Dox for 2 hr. Bottom: WB of the same gel with anti-Myc Ab.

B: HCT116 cells transfected with Myc-Che-1 or the indicated Che-1 mutants. At 48 hr posttransfection, cells were treated with 1 μM Dox and 20 μM chx for the indicated times and analyzed by WB with the indicated Abs.

C: WB of HCT116 and HCT15 cells treated with the indicated drugs for 2 hr (1 μM Dox, 10 mM caffeine).

D: AT fibroblasts transfected with nonspecific control pool (control) or with SMART pool Chk2 siRNAs. At 48 hr posttransfection, cells were treated with 1 μM Dox and TCEs analyzed by WB with the indicated Abs.

E: TCEs from HCT116 cells untransfected (left) or transfected with Myc-Che-1 or Myc-Che-1^{S4A} mutant (right) and treated with 1 μM Dox for 1 hr were analyzed by WB with anti-P-Ser141 Ab (top panels). The same filters were assessed with anti-Che-1 (bottom left) or anti-Myc (bottom right) Abs. Bottom panel: Che-1 phosphopeptide sequence to produce the phospho-specific antiserum.

by restoring the expression of wild-type, but not of kinase-dead, Chk2 (Figure 3B). Compatible results were obtained in HCT116 cells upon Chk2 depletion by siRNA (Figure S2D), strongly suggesting that Chk2 contributes to Che-1 half-life regulation.

Next, we performed a series of experiments similar to those described above for the ATM/Che-1 interaction to test the physical and functional interaction between Che-1 and Chk2. Coimmunoprecipitation of endogenous proteins was performed in untreated and Dox-treated HCT116 cells with anti-Chk2 Ab. A strong interaction between Che-1 and Chk2 was detected after DNA damage (Figure 3C) and confirmed in U2OS cells transfected with Myc-Che-1 and Flag-Chk2 and treated with Dox or IR (Figure S2E).

To evaluate the ability of Chk2 to phosphorylate Che-1, recombinant GST-Che-1 was used as substrate for immunoprecipitated Myc-Chk2 in in vitro kinase assay. As shown in Figure 3D, Che-1 was phosphorylated by Chk2 as efficiently as p53. Three putative Chk2 phosphorylation sites (Stevens et al., 2003) are present in Che-1 at resides Ser141, Ser474, and Ser508. Thus, we performed in vitro Chk2 kinase assays utilizing the GST-Che-1 fusion peptides spanning these residues as substrates. Both GST-84-173 and GST-471-558 were phosphorylated (Figure S3F), suggesting that Chk2 targets more than one residue on Che-1. Accordingly, the phosphorylation of Che-1 with double Ser-to-Ala mutations at residues 141 and 474 (Myc-Che-1$^{S141A/S474A}$) or 141 and 508 (Myc-Che-1$^{S141A/S508A}$) was markedly attenuated, whereas the phosphorylation of Che-1 with a triple mutation (Myc-Che-1^{S3A}) was abrogated (Figure 3E), and Dox treatment almost failed to increase the half-life of this mutant (Figure 3F). Taken together, these results indicate that Chk2 phosphorylates Che-1 and this phosphorylation contributes to increase Che-1 stability.

Since Chk1 and Chk2 share most of their known substrates (Bartek and Lukas, 2003), we tested whether Chk1 can phosphorylate Che-1. A kinase assay was performed with immunoprecipitated Flag-Chk1 from transfected 293 cells. GST-Che-1 was strongly phosphorylated by Chk1 (Figure 3G), suggesting that this kinase might also affect Che-1 stabilization.

ATM and Chk2 cooperate to stabilize Che-1

The above observations suggest that ATM/ATR and Chk2 are required for increasing Che-1 stability in DDR. To test this hypothesis, a Che-1 mutant lacking both ATM and Chk2 phospho-sites (Myc-Che-1^{S4A}) was constructed and tested for in vivo phosphorylation and stability. After Dox treatment of ^{32}P-orthophosphate-labeled HCT116 cells, the wild-type Myc-Che-1 was strongly phosphorylated while the Myc-Che-1^{S4A} mutant was not (Figure 4A), indicating that the S4A mutant is no longer phosphorylated in vivo upon DNA damage. Next, we compared the half-lives of the different Che-1 mutants by WB in the presence of Chx. A progressive reduction of the half-life was detectable with the ATM/ATR-unphosphorylatable Che-1^{S187A} single mutant being the most stable, though less than the wild-type Che-1 and the Che-1^{S4A}, which are completely resistant to stabilization (Figure 4B, compare the uppermost and lowest lanes of Figure 4B). In agreement, inhibition of ATM/ATR activity by caffeine in Chk2-defective HCT15 cells and Chk2 depletion by siRNA in ATM$^{-/-}$ cells completely abrogated the Dox-induced Che-1 stabilization (Figures 4C and 4D).

To evaluate whether endogenous Che-1 is phosphorylated at these sites in vivo, we produced an anti-phospho-specific peptide antiserum directed against the phosphorylated Ser141 (P-Ser141; Figure 4E). The other three sites could not be employed for technical reasons (for details, see Experimental Procedures). The anti-P-Ser141 Ab strongly reacted with Che-1 after Dox treatment and did not show any reactivity on the Myc-Che-1^{S4A} mutant (Figure 4E).

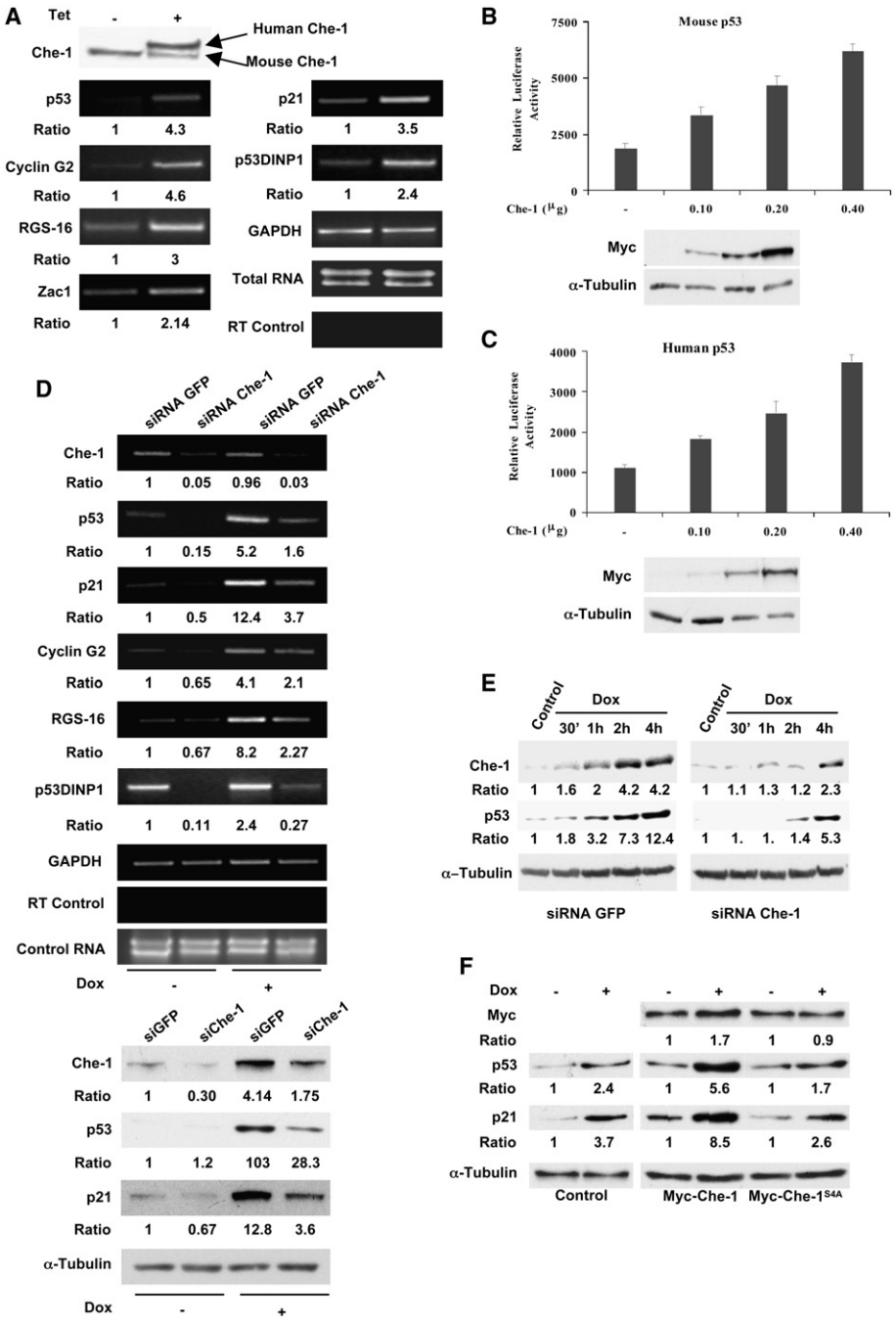

Figure 5. Che-1 activates p53 transcription

A: Equal amounts of RNA (RNA input) from NIH3T3 cells uninduced (−Tet) and induced (+Tet) to express Che-1 were analyzed by RT-PCR (25–30 cycles) for expression of the indicated genes. The RT control lanes represent RT-PCR in the absence of reverse transcription.

B and C: HCT116 cells were transiently transfected with 1 μg of the indicated luciferase reporters and, where indicated, with increasing amounts of Myc-Che-1 expression vector. Lower panels: Myc-Che-1 expression by WB with anti-Myc Ab. Error bars indicate SD.

D: HCT116 cells were transiently transfected with siRNA GFP (siGFP) or siRNA Che-1 (siChe-1) and 48 hr later treated, where indicated, with 1 μM Dox for 2 hr. Top: RT-PCR evaluates the expression of the indicated genes. Bottom: WB with the indicated Abs.

E: WB with the indicated Abs of TCEs from HCT116 transfected as in **D** and treated 48 hr later with 1 μM Dox for the indicated times.

F: WB of HCT116 cells untransfected (control) or transfected with Myc-Che-1 or Myc-Che-1^{S4A} mutant and treated or not with 1 μM Dox for 2 hr.

Che-1 activates p53 transcription

The data described above demonstrate that DDR is associated with ATM/ATR- and Chk2-mediated accumulation of Che-1. Since Che-1 is a RNA Pol II-binding protein involved in gene transcription, to understand the biological relevance of Che-1 accumulation in DDR, we used high-density Affimetrix microarrays. Messenger RNA was extracted from NIH3T3 cells that conditionally express human Che-1 cDNA in a tetracycline (Tet)-regulated manner (Bruno et al., 2002). Both noninduced and Tet-induced cells were employed. Transcriptional profiles were compared and computational analyses performed to identify genes regulated only after Che-1 overexpression. In agreement with previous results (Bruno et al., 2002), several E2F target genes (Muller et al., 2001) were found to be induced by Che-1 (data not shown). Interestingly, among the Che-1-induced genes we identified the *TP53* oncosuppressor, whose role in DDR is well established (Wahl and Carr, 2001), several p53 targets, e.g., *p21, MDM2*, *cyclin G2, P53DINP1* (Levine, 1997; Okamoto and Beach, 1994; Buckbinder et al., 1997; Okamura et al., 2001), and the p53 coactivator *Zac1* (Huang et al., 2001). These microarray data were confirmed by semiquantitative RT-PCR (Figure 5A). Furthermore, luciferase reporter assays showed a dose-dependent activation of the human and mouse *TP53* promoters by Myc-Che-1 overexpression (Figures 5B and 5C).

To evaluate whether Che-1-mediated regulation of these genes is preserved following DDR, HCT116 cells were depleted

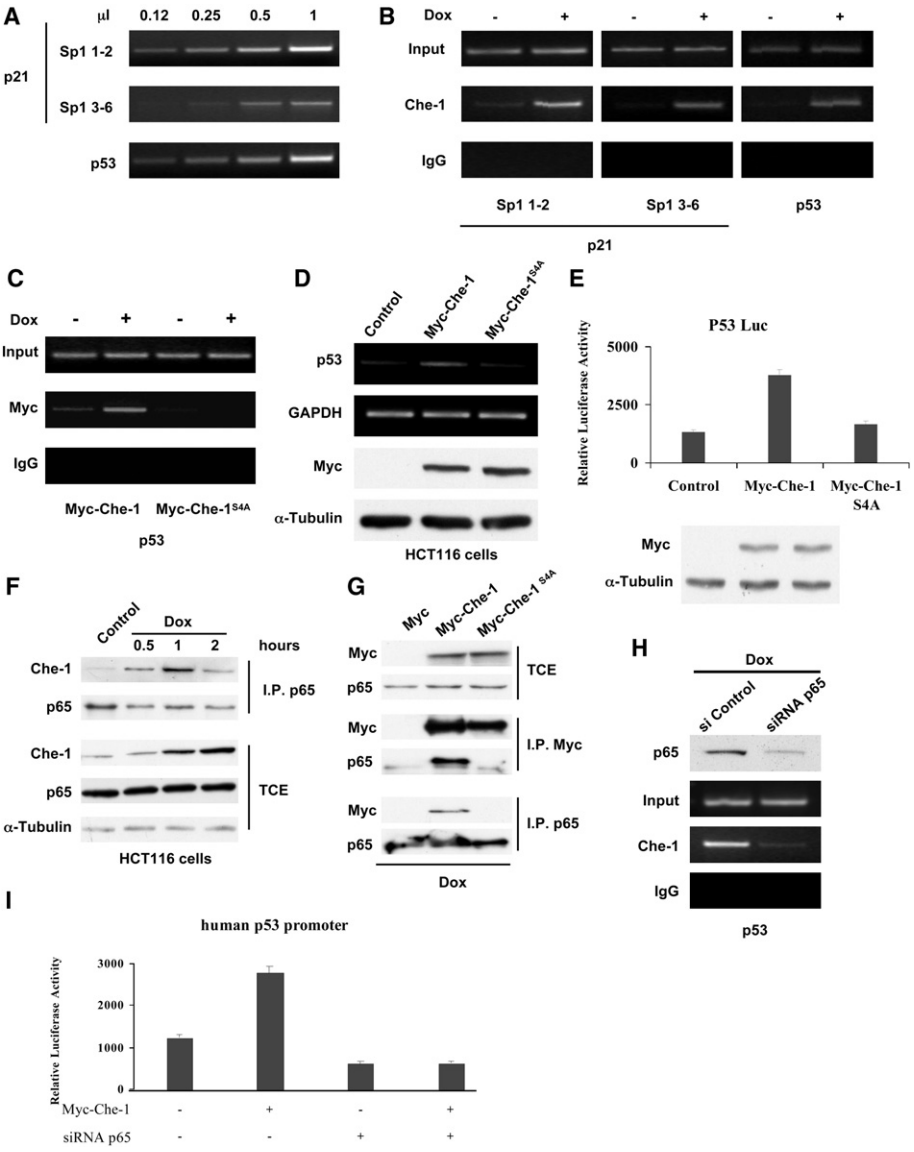

Figure 6. DNA damage promotes Che-1 recruitment on *p21* and *Tp53* promoters

A: Increasing amounts of input samples (0.12, 0.25, 0.5, 1 μl) were used as template in PCR amplifications with specific primers for the indicated promoters.

B: TCEs from HCT116 cells treated (+) or not (−) with 1 μM Dox for 2 hr were subjected to ChIP using anti-Che-1 Ab. Immunoprecipitates from each sample were analyzed by PCR and a sample representing linear amplification (0.2–0.4 μl) of the total input chromatin (Input) was included in the PCRs as a control. Additional control included a precipitation performed with nonspecific IgGs.

C: HCT116 cells were transfected with Myc-Che-1 or Myc-Che-1^{S4A} and treated (+) or not (−) with 1 μM Dox for 2 hr. TCEs were subjected to ChIP with anti-Myc Ab.

D: Equal amounts of RNA (RNA input) from HCT116 transfected with the indicated expression vectors were analyzed by RT-PCR (25–30 cycles) for the expression of the indicated genes.

E: HCT116 cells were transiently transfected with 1 μg of *TP53* promoter luciferase reporter and, where indicated, with 1 μg of Myc empty vector (control), Myc-Che-1, and Myc-Che-1^{S4A} expression vectors. Lower panels, the expression levels of Myc tagged Che-1 were assayed by WB with anti-Myc Ab. Error bars indicate SD.

F: TCEs from HCT116 cells treated for the indicated times with 1 μM Dox were immunoprecipitated with anti-p65 Ab and analyzed by WB with the indicated Abs.

G: HCT116 cells were transfected with WT Myc-Che-1 or Myc-Che-1^{S4A} mutant. At 48 hr post-transfection, cells were treated with 1 μM Dox for 1 hr. TCEs were immunoprecipitated with anti-p65 or anti-Myc Abs and analyzed by WB with the indicated Abs.

H: HCT116 cells were transiently transfected with Smart-Pool siRNA (si Control) or p65 siRNA (si p65) and 48 hr later treated, where indicated, with 1 μM Dox for 2 hr. Then, cells were subjected to ChIP using anti-Che-1 Ab or no IgGs.

I: HCT116 cells were transiently transfected with 1 μg of the human *TP53* promoter luciferase reporter, Smart-Pool siRNA (−) or p65 siRNA (+), and Myc-Che-1, where indicated. Error bars indicate SD.

of Che-1 expression by siRNA (Figure 5D, uppermost panel) and tested by RT-PCR in the presence or absence of Dox. As expected, Dox treatment did not increase *Che-1* mRNA levels, confirming that DDR regulates Che-1 only at the posttranslational level (Figure 5D, uppermost panel). Che-1 depletion significantly inhibited transcription of the *TP53* gene and all the other genes identified in the microarray both in basal condition and upon Dox treatment (Figure 5D and Figure S3D), supporting a role of Che-1 in their transcriptional regulation. The inhibition of p53 and p21 expression was also verified at the protein level (Figure 5D, lowest panels). Indeed, despite the strong and well characterized p53 stabilization induced by posttranslational modifications in DDR, time course analysis showed that Che-1 depletion significantly delayed p53 accumulation (Figure 5E), strongly indicating that Che-1 contributes to p53 induction. In addition, time course analyses of Tet-induced and -uninduced NIH3T3 cells treated with Dox confirmed that Che-1 affects p53 expression (Figure S3A), and comparable results were obtained when Myc-Che-1-overexpressing HCT116 cells were treated with Dox (Figure S3B).

Finally, we compared the effect of wild-type Che-1 and the nonphosphorylatable Che-1^{S4A} mutant on p53 and p21 expression in the absence or presence of Dox. The exogenous expression of either Che-1 protein in the absence of Dox increased the expression of p53 and p21 to a similar extent. However, upon Dox treatment, only the wild-type Che-1, which can be phosphorylated and stabilized, further and strongly increased p53 and p21 expression (Figure 5F), indicating that the phosphorylation of Che-1 contributes to the activation of these genes.

DNA damage promotes Che-1 recruitment on the *TP53* and *p21* promoters

Che-1 can be immunoprecipitated with the chromatin of E2F target genes during the G_1/S transition (Bruno et al., 2002). To evaluate whether Che-1 is present on the *TP53* and *p21* promoters in

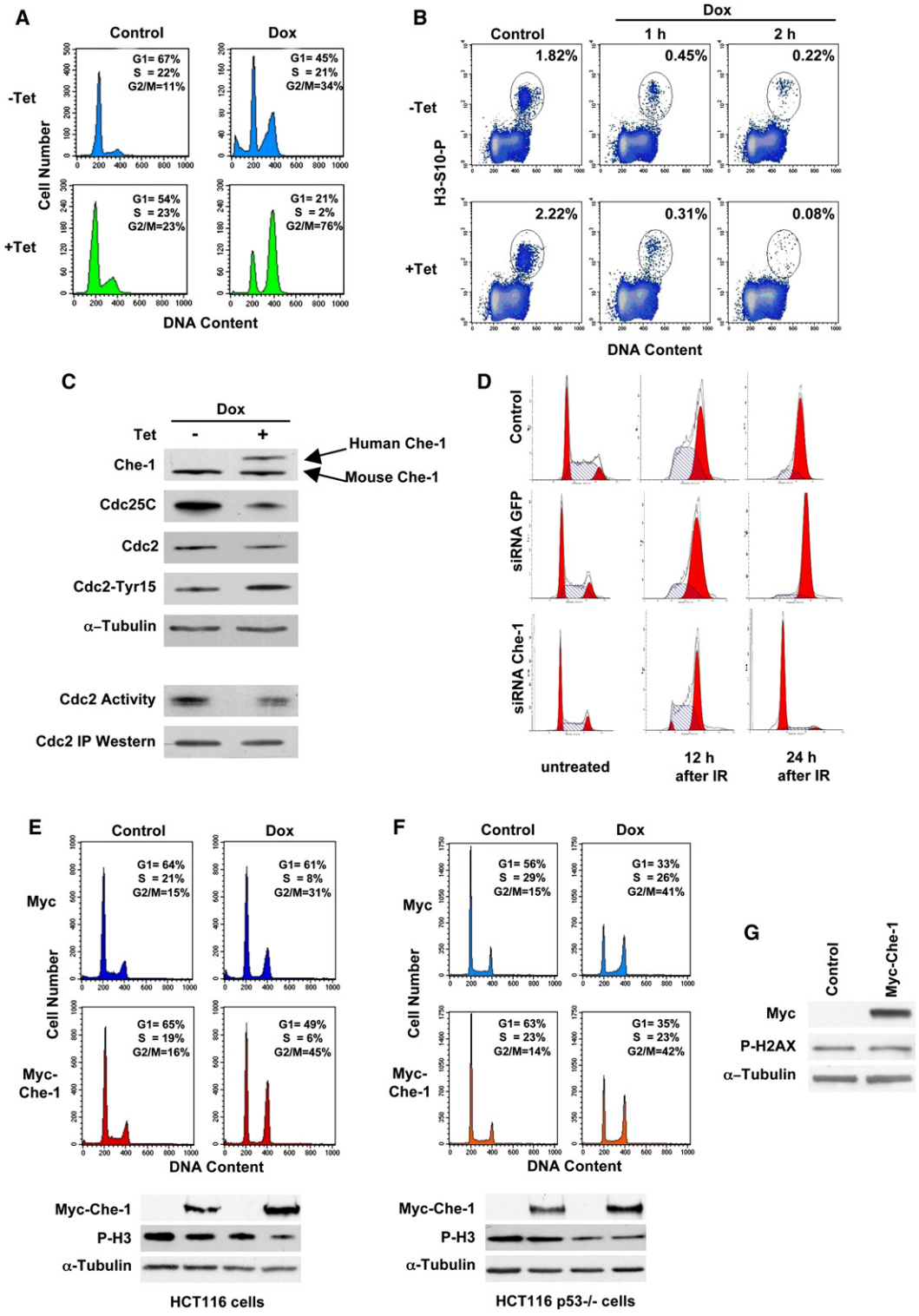

Figure 7. Che-1 is involved in G_2/M checkpoint maintenance

A: NIH3T3 cells induced (+Tet) or not (−Tet) were treated with or without 0.5 μM Dox for 24 hr. Cells were then fixed and stained with propidium iodide (PI) and analyzed for DNA content.

B: Cell-cycle profiles of −Tet and +Tet NIH3T3 cells treated with 1 μM Dox for the indicated times. Profiles were determined by flow cytometry, which monitored phosphorylation of histone H3 at Ser 10 (H3-S10-P), and DNA content by PI staining.

C: Top: NIH3T3 cells induced (+Tet) or not (−Tet) were treated with 1 μM Dox. TCEs were analyzed by WB with the indicated Abs. Bottom: Cdc2/Cyclin B1 complex was immunoprecipitated with anti-cyclin B1 Ab and assayed for kinase activity using histone H1 substrate (see Experimental Procedures). The amount of Cdc2 protein in the immunocomplexes was assessed by WB.

D: FACS profile of untransfected, GFP-siRNA-, and Che-1-siRNA-transfected 293 cells either untreated or subjected to IR (6 Gy) and stained with PI at the indicated times.

DDR, chromatin immunoprecipitations (ChIP) were performed analyzing the NF-κB-binding region of the *TP53* promoter (Hellin et al., 1998; Pei et al., 1999) and the Sp1-binding regions of the *p21* promoter (Di Padova et al., 2003). As shown in Figure 6B, ChIPs carried out under conditions of linear amplification (Figure 6A) revealed that the amount of Che-1 physically associated with the *TP53* and *p21* promoters was barely detectable in normal proliferating conditions but drastically increased after Dox treatment. Interestingly, a concomitant reduction of the amount of Che-1 on the promoters of E2F target genes *Dhfr* and *cyclin A* was observed, indicating that in DDR, Che-1 is displaced from E2F target genes and recruited on the *p21* and *TP53* promoters (Figure S3C). To evaluate whether the recruitment of Che-1 on the *TP53* promoter is mediated by ATM/ATR and Chk2 phosphorylation, HCT116 cells expressing Myc-Che-1 wild-type or the Myc-Che-1^{S4A} mutant were treated with Dox and subjected to ChIP with anti-Myc Ab. The amount of Myc-Che-1 on the *TP53* promoter was strongly increased by Dox treatment, whereas Myc-Che-1^{S4A} was only barely detectable on this promoter in both untreated and Dox-treated cells (Figure 6C). Conversely, Myc-Che-1^{S4A} was found associated to *DHFR* promoter, and DNA damage displaced it to a lesser extent than Myc-Che-1 wild-type (Figure S3C). These results were confirmed when Luc reporter of *TP53* promoter was transfected into HCT116 cells with Myc-Che-1 or Myc-Che-1^{S4A}. Indeed, the mutant form of Che-1 did not activate *TP53* transcription or Luc reporter of *TP53* promoter (Figures 6D and 6E), while it did activate the E2F-target genes as well as the wild-type Che-1 (data not shown).

Next, we tried to identify the mechanism(s) that allows Che-1 to target the *TP53* promoter in DDR, and to determine whether this function is regulated by Che-1 phosphorylation. Che-1 does not directly bind DNA (Fanciulli et al., 2000); therefore, we investigated whether this molecule could form new interactions with specific transcription factors in DDR. NF-κB binds the *TP53* promoter in DDR and regulates its activation (Hellin et al., 1998; Pei et al., 1999); thus, we tested whether Che-1 and the NF-κB p65 subunit can physically and functionally interact. As shown in Figure 6F, coimmunoprecipitation of Che-1 with anti-p65 Ab demonstrated increased amounts of Che-1 associated to p65 after DNA damage. To test whether Che-1 phosphorylation was required for this interaction, coimmunoprecipitation experiments were performed with HCT116 cells transfected with Myc-tag empty vector, Myc-Che-1, or Myc-Che-1^{S4A} and treated with Dox. As shown in Figure 6G, Myc-Che-1 strongly interacted with p65 whereas Myc-Che-1^{S4A} did not bind this protein, indicating that Che-1 phosphorylation regulates Che-1/p65 interaction. Next, we tested whether p65 recruits Che-1 on the *TP53* promoter by ChIP analysis performed after DNA damage in the presence or absence of p65-specific siRNA (Figure 6H). The amount of Che-1 on the *TP53* promoter strongly decreased in the absence of p65 (Figure 6H). Furthermore, upon p65 depletion, Che-1 did not activate *TP53* transcription (Figure 6I). Taken together, these observations strongly suggest that Che-1 phosphorylation in DDR can regulate protein-protein interactions and confer promoter specificity.

Che-1 is involved in the maintenance of the G_2/M checkpoint

Based on the results we obtained thus far, we asked whether Che-1 is involved in the regulation of G_1/S and G_2/M checkpoints in response to Dox treatment. The NIH3T3 cells that conditionally express human Che-1 were employed. The Tet-induced, Che-1-overexpressing cells exhibited a cell-cycle profile with a strong G_1 depletion and a concomitant G_2/M accumulation (Figure 7A), suggesting that Che-1 is involved in the G_2/M transition checkpoint. Consistently Che-1-overexpressing cells showed a marked reduction in the levels of Ser10-phosphorylated H3 histone, a typical mitosis marker (Wei et al., 1999) (Figure 7B), and of Cdc25C phosphatase, a dual specific phosphatase whose activity is essential for entry into mitosis (Dunphy, 1994) (Figure 7C), as well as increased amounts of Cdc2-Tyr15 phosphorylation, a key target of Cdc25C (Morla et al., 1989), correlated with a reduced Cdc2 kinase activity (Figure 7C).

To further confirm the involvement of Che-1 in the G_2/M checkpoint, 293 cells were transfected with shRNA-pSuper vectors silencing Che-1 or GFP and exposed to IR followed by cell-cycle analysis. Both Che-1-depleted and control cells (untransfected or GFP shRNA transfected) exhibited a G_2 arrest; however, at later time points (24 hr) most of the Che-1-depleted cells entered G_1 while controls remained arrested in G_2 (Figure 7D), indicating a failure of the Che-1-depleted cells to maintain the G_2 arrest. In addition, Che-1 overexpression induced in HCT116 and HCT116 $p53^{-/-}$ cells produced an increase of G_2/M accumulation only in the p53-proficient cells (Figures 7E and 7F), indicating the p53-dependance of this phenomenon. Indeed, although the $p53^{-/-}$ cells have a completely different checkpoint activation by Dox treatment, as expected (Bunz et al., 1998), Che-1 overexpression was not able to modify their cell-cycle profile (Figure 7F).

Finally, we tested whether Che-1 overexpression can cause DNA damage by itself. Myc-Che-1 or empty expression vectors were transfected into HCT116 cells, and the levels of phosphorylated histone H2AX were examined in the absence of drug. As shown in Figure 7G, Che-1 did not affect phosphorylation of histone H2AX, indicating that Che-1 overexpression does not cause replication stress that activates DDR. Taken together, these results strongly support an involvement of Che-1 in the maintenance of the G_2/M checkpoint in DDR.

Che-1 depletion increases sensitivity to anticancer agents

In DDR, Che-1 is stabilized by its phosphorylation and contributes to the G_2/M checkpoint by p53 and p21 activation. Therefore, we asked whether Che-1 expression affects tumor cell sensitivity to DNA-damaging drugs. HCT116 cells were transfected with wild-type Che-1 or the nonphosphorylatable Che-1^{S4A} mutant and treated with Dox. Wild-type Che-1 strongly protected cells from apoptosis, whereas the mutant was significantly less effective (Figures 8A and 8B), indicating that Che-1 phosphorylation is required for its antiapoptotic activity. Notably, Che-1 overexpression did not protect HCT116 $p53^{-/-}$ cells (Figure 8C), supporting the requirement of p53 for Che-1 antiapoptotic

E and F: $p53^{+/+}$ (**E**) or $p53^{-/-}$ (**F**) HCT116 cells were treated with or without 0.5 μM Dox for 24 hr. Top: Cells were fixed, stained with PI, and analyzed for DNA content. Bottom: TCEs were blotted and analyzed with the indicated Abs.
G: WB of HCT116 cells transfected either with Myc-tag empty vector or Myc-Che-1.

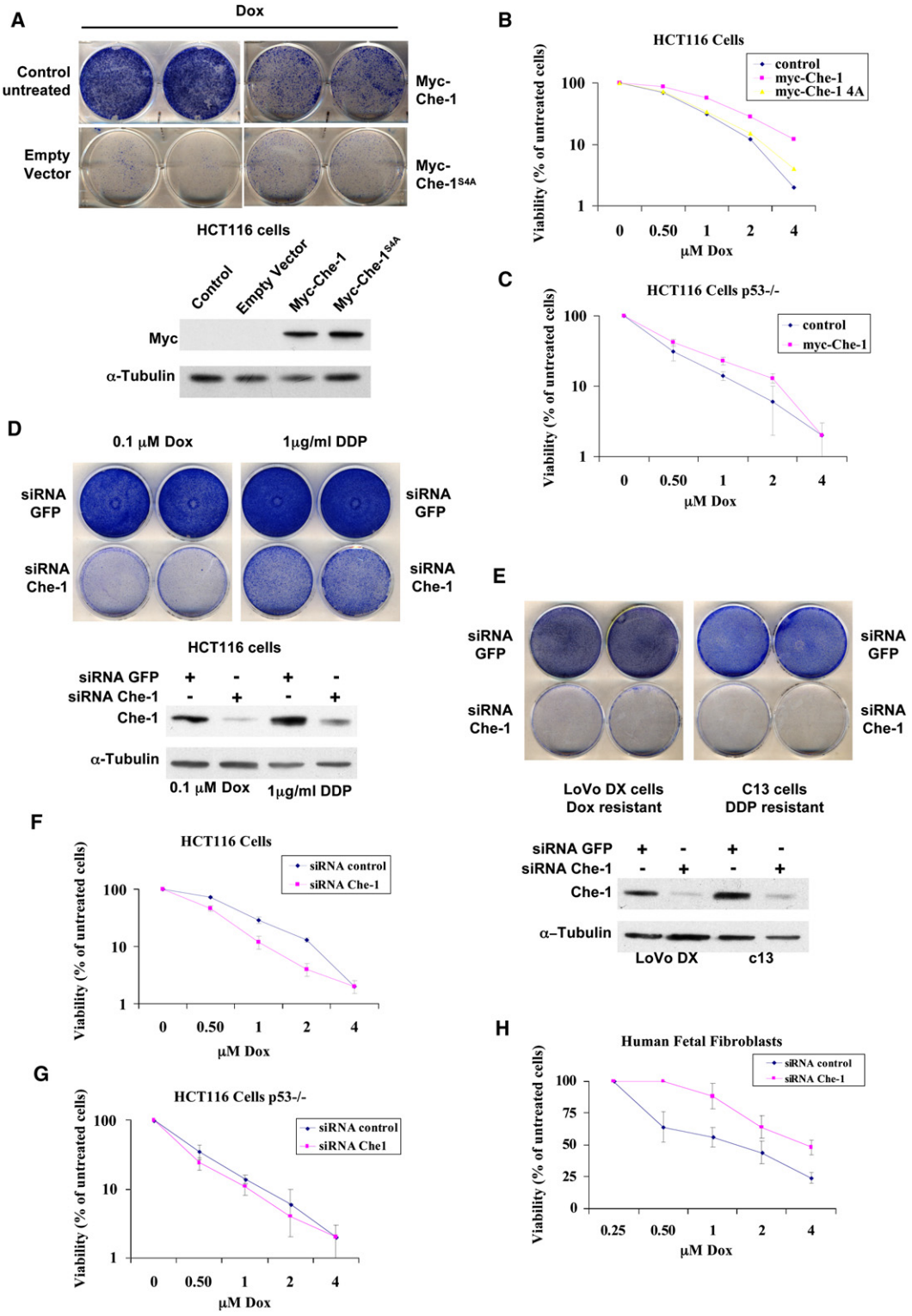

Figure 8. Che-1 depletion sensitizes tumor cells to anticancer drugs

A: Top: HCT116 cells were transiently transfected with Myc-tag empty vector, Myc-Che-1, and Myc-Che-1^{S4A} expression vectors. At 48 hr posttransfection, cells were treated with 1 μM Dox for 12 hr. After 7 days, parallel plates were stained with methylene blue. Bottom: expression levels of Myc-Che-1 by WB with anti-Myc Ab.

B and C: Colony-formation assay performed with p53$^{+/+}$ (**B**) and p53$^{-/-}$ (**C**) HCT116 cells transfected with the indicated plasmids, exposed to the indicated doses of Dox for 12 hr, and evaluated 7 days later. The clonogenic assays were performed in triplicate. Error bars indicate SD.

D: Top: HCT116 cells were transiently transfected with siRNA GFP or siRNA Che-1 and 48 hr later treated, where indicated, with sublethal doses of Dox or DDP for 12 hr. After 7 days cells were treated as in **A**. Bottom: expression level of Che-1 and α-tubulin were assayed by WB.

activity. Conversely, Che-1 depletion by siRNA strongly increased Dox cytotoxicity (Figure 8F) and induced apoptosis in HCT116 cells treated with sublethal doses of Dox or DDP (Figure 8D). In addition, Che-1 inhibition reverted chemoresistance in colon cancer LoVo DX and ovarian cancer c13 cells, resistant to Dox and DDP, respectively (Figure 8E). Comparable results were obtained with other Dox-resistant cells (breast cancer MCF7 and melanoma M14; data not shown). In agreement with previous results (Figure 8C), Che-1 depletion did not significantly affect HCT116 p53$^{-/-}$ cells (Figure 8G and Figure S4A). Next, we evaluated whether normal HFFs were sensitized to Dox by Che-1 removal. Che-1 depletion strongly reduces HFF proliferation (Bruno et al., 2002) and protected these cells from drug treatment (Figure 8H). Taken together, these results indicate that Che-1 defends cells from apoptosis in a p53-dependent manner and that its depletion sensitizes tumor but not normal cells to anticancer drugs.

Discussion

Eukaryotic cells' DDR involves the activation of ATM/ATR kinases that can specifically target p53 for phosphorylation, either directly or indirectly through Chk2 and Chk1 kinases. These p53 modifications are required for inhibiting p53 degradation by MDM2 and for allowing additional p53-activating posttranslational modifications. Here, we show that ATM and Chk2 can also modulate *TP53* and *p21* gene transcription through phosphorylation of the transcription regulator Che-1. Moreover, we show that Che-1 contributes to the maintenance of the G_2/M checkpoint and that its downregulation by siRNA sensitizes cancer cells to chemotherapy.

Our results show that Che-1 is stabilized in vitro and in vivo in response to either physical and chemical genotoxic agents. This induction is very rapid (within 45 min from damage) and is mediated by posttranslational modifications. In vivo phosphate metabolic labeling and anti-phospho-Che-1 Ab revealed that Che-1 is strongly phosphorylated in DDR. In addition, we found that Che-1's half-life is regulated by the proteasome and that specific phosphorylations protect the protein from degradation.

We show that ATM and Chk2 kinases can phosphorylate Che-1, increasing its half-life and contributing to activation of p53 and p21 at the transcriptional level and to maintenance of the G_2/M checkpoint. Although multiple phosphorylations are necessary for a complete phenotype, our results showed that both ATM and Chk2 alone posses measurable effects on Che-1 stabilization. Furthermore, we demonstrate that other kinases involved in DDR, such as ATR and Chk1, phosphorylate Che-1, thus suggesting that this modification is a general event following DNA damage.

We have previously reported that Che-1 is involved in the activation of E2F-target gene promoters and cell proliferation affecting Rb growth suppression (Fanciulli et al., 2000; Bruno et al., 2002), and that Che-1 is found on the E2F target gene promoters during the G_1/S transition (Bruno et al., 2002). Here we show that treatment with Dox increases the selective recruitment of Che-1 on the *TP53* and *p21* promoters. Moreover, Che-1 phosphorylation by ATM and Chk2 is required for Che-1 recruitment on the *TP53* promoter, whereas it does not affect Che-1 recruitment onto E2F-target gene promoters (data not shown). It has been described that DNA damage activation of the *TP53* promoter is mediated by NF-κB (Hellin et al., 1998; Pei et al., 1999). Accordingly, we show here that Dox treatment markedly increases Che-1 levels at the NF-κB site of the human *TP53* promoter. Che-1 interacts with the NF-kB subunit p65; this interaction is mediated by Che-1 phosphorylation and is increased in DDR. Therefore, it is possible that posttranslational modifications of Che-1 mediate its interactions with transcription factors or cofactors and in such way regulate Che-1's presence onto specific promoters.

Che-1 was found to activate p53 transcription in the absence of DNA damage (Figures 5A–5C), but even in this case p53 transactivation requires Che-1 phosphorylation (Figures 6D and 6E). Consistent with these findings, Che-1 phosphorylation is also slightly detectable even in absence of Dox treatment (Figure 1G), probably by intrinsic DNA damage occurring during DNA replication or by another mechanism(s) to be characterized. Thus, it is possible to speculate a model where Che-1 is required for the basal state of p53 expression, and that this effect is preserved and reinforced in DDR.

We show that Che-1 is involved in the maintenance of the G_2/M checkpoint, at least in part, by activation of the *TP53* and *p21* genes. The products of these genes were characterized as key proteins in the regulation of both G_1 and G_2 checkpoints (Wahl and Carr, 2001; Boulaire et al., 2000); therefore, the Che-1 effects in the G_2/M checkpoint might be paradoxical. However, a way to reconcile these data is to point out that one of the key functions of Che-1 is to promote E2F gene transcription by displacing HDAC1 from Rb, weakening in this way p53's effects on the G_1 checkpoint. On the other hand, evidence implicates p53 and p21 in controlling entry into mitosis when cells enter G_2 with damaged DNA (Bunz et al., 1998; Taylor and Stark, 2001).

We recently showed that Che-1 is downregulated in several tumors and that Che-1 overexpression arrests the growth of human colon carcinoma cell lines through a p53-independent induction of p21 (Di Padova et al., 2003). This observation fits with a model where Che-1 is considered a component of DDR that protects cells from early progression of human cancer (Bartkova et al., 2005; Gorgoulis et al., 2005). Furthermore, the early embryonic lethality of Che-1-deficient mice (Thomas et al., 2000) suggests that Che-1 as well as ATR and Chk1 could be required for normal progression through the cell cycle, even in absence of cellular stress.

DNA-damaging agents are the mainstays of cancer therapy and have achieved impressive clinical results. However, they are often plagued by various limitations, such as elevated systemic toxicity or drug resistance. Activation of DNA damage checkpoints promotes DNA repair and cell survival, but it might also reduce the effectiveness of chemotherapeutics. Therefore,

E: Top: LoVo DX (Dox-resistant) and c13 (DDP-resistant) cells were transiently transfected with siRNA GFP or siRNA Che-1 and grown in the presence of 0.5 μM Dox (LoVo DX) or 5 μg/ml DDP (c13). After 7 days cells were treated as in **A**. Bottom: expression level of Che-1 and α-tubulin were assayed by WB.
F–H: HCT116 (**F**), HCT116 p53$^{-/-}$ (**G**), and HFF (**H**) cells were transfected with siGFP (siRNA control) or siChe-1 and subjected to colony-formation assays after Dox treatments as described in **B**. Error bars indicate SD.

the cytotoxicity of unspecific DNA-damaging agents that normally induce cell-cycle arrest in tumor cells could be enhanced by combining them with checkpoint inhibitors (Zhou and Bartek, 2004). In agreement with these considerations, our studies confirm that Che-1 is an antiapoptotic factor (Page et al., 1999) and demonstrate that Che-1 phosphorylation is required for this activity. More importantly, they show that Che-1 inhibition intensifies the cytotoxicity of anticancer drugs that damage the DNA and, in such way, can revert chemoresistance of several tumor cell lines. Conversely, in normal cells, with more intact cell-cycle control, the lack of Che-1 function in DDR is better tolerated. The latter observation strengthens the notion that Che-1 can be considered a valid target for the design of drugs that can enhance the efficacy of chemotherapeutic drugs in cancer patients without cytotoxicity on their own.

Experimental procedures

Cell culture, transfections, and analysis

$p53^{+/+}$ and $p53^{-/-}$ HCT116 and MEF, 293, and NIH3T3 expressing Tet-conditional Che-1 (Bruno et al., 2002) were grown in DMEM supplemented with 10% fetal bovine serum (FBS); HFF and ATM $^{-/-}$ human fibroblasts (AT) (a kind gift from Dr. L. Wood) with 15% FBS; HCT15 cells were grown in RPMI plus 15% FBS. U2OS, LoVo DX (Dox-resistant cells), and c13 (DDP-resistant cells) (kindly provided by Dr. Howell) were grown in RPMI plus 10% FBS. HCT15 cells stably transfected with either wild-type Chk2 or kd Chk2 were kindly provided by Dr. J. Chen. Flow cytometric analyses were performed using FACScalibur (Becton-Dickinson, San Jose, CA). Data analyses were performed using Cell Quest (BDIS) and ModFit LT (Verity Software House, Topsham, ME). Transfections were carried out by BES-calcium phosphate precipitation as described (Fanciulli et al., 2000) or by Lipofectamine Plus (Invitrogen). Colony-forming efficiency assays and luciferase assays were performed as previously described (Fanciulli et al., 2000). Data are presented as mean ± SD of three independent experiments performed in duplicate. Doxorubicin, caffeine, and cycloheximide were purchased from Sigma, whereas MG132 was purchased from Calbiochem. Clinical-grade DDP (Cisplatino Teva) was obtained from Teva Pharma.

Recombinant plasmids and proteins

The Myc-tagged Che-1 and its deletions were described (Fanciulli et al., 2000). Che-1 deletions were cloned into the pGEX4T3 vector (Pharmacia) to produce Glutathione-S-transferase (GST) fusion proteins. Plasmids expressing bacterial recombinant GST-p53 and 6×His-p53 were produced by cloning the complete ORF of mouse p53 into pGEX4T1 (Pharmacia) or pQE30 (QIAGEN) bacterial expression vectors, respectively. Flag-ATM and Flag-ATM kd expression vectors were kind gifts from Dr. Y. Shiloh and Dr. M.B. Kastan, respectively. Flag-ATR and Flag-ATR kd expression vectors were kindly provided by Dr. Okamoto. Myc-Chk2, Myc-Chk2 kd, and Flag-Chk1 were a gift from Dr. J. Bartek. The human and mouse *p53* promoters fused to luciferase reporter were kindly provided by Dr. M. Oren and Dr. V. Rotter. GST-tagged proteins were produced as described (Fanciulli et al., 2000). Mutagenesis of Myc-Che-1 was performed using the QuikChange Mutagenesis system (Stratagene).

Antibodies

The following rabbit polyclonal Abs were used: anti-Che-1 (Fanciulli et al., 2000), p53, p65, Cdc2, (Tyr-15)-P-Cdc2, Cdc25C, (sc-6243, sc-372, sc-954, sc-7989, sc-327; Santa Cruz), Cyclin B1 (Calbiochem), and anti-(Ser10)-P-histone H3 (Upstate). Mouse monoclonal Abs anti-Myc 9e10 (Invitrogen), Flag M2 (Sigma), anti-P-histone H2AX and Chk2 (Upstate), ATM (Delia et al., 2000), α-tubulin, and human p21 (sc-8035 and sc-6246; Santa Cruz) were also used.

Immunoprecipitations and WB analysis

TCEs were immunoprecipitated by standard procedures. WB were prepared by standard procedures, and immunoreactivity was detected by ECL chemioluminescence reaction (Amersham). Densitometric analyses of immunoblots and RT-PCR were performed using Quantity-One software (Bio-Rad). Ratios were calculated by the following formula:

$$\frac{\text{intensity sample}/\text{intensity } \alpha\text{-tubulin (or GAPDH)}}{\text{intensity control}/\text{intensity } \alpha\text{-tubulin (or GAPDH)}}.$$

Metabolic labeling

Cells were incubated for 2 hr with 0.5 mCi/ml [^{32}P] inorganic phosphate (Amersham) in phosphate-free medium (Sigma), in presence of absence of Dox, before immunoprecipitation of Che-1 with the indicated Abs. For pulse-chase analysis, cells were incubated for 1 hr with or without Dox and then with 0.5 mCi/ml [^{35}S] methionine (Amersham) in DMEM without methionine (Sigma) for 20 min. Then, cells were extensively washed, incubated in DMEM medium, and collected at the indicated times. TCEs were immunoprecipitated with anti-Che-1 Ab.

Kinase assays

Immunoprecipitated Flag-ATM, Flag-ATR, Myc-Chk2, and Flag-Chk1 were incubated with GST fusion proteins in kinase buffer (see Supplemental Data) for 30 min at 30°C. Kinase assays for Cdc2 were carried out by incubating immunoprecipitated Cdc2/cyclin B1 complex and 1 μg of Histone H1 (Sigma) as substrate in Cdc2 kinase buffer. Reactions were stopped by adding 5× sample buffer, and proteins were resolved by SDS-PAGE. Dried gels were analyzed by phosphoimager (Bio-Rad).

Chromatin immunoprecipitation assay

Chromatin immunoprecipitation (ChIP) assays were performed using anti-Che-1 polyclonal Ab as described (Bruno et al., 2002). In each experiment, signal linearity was ensured by amplifying increasing amounts of template DNA (see Figure 6A). Generally, DNA representing 0.005% to 0.01% of the total chromatin sample (input) or 1% to 10% of the immunoprecipitated was amplified using promoter-specific primers whose sequences are provided in Supplemental Data. Immunoprecipitations with no specific immunoglobulins (Santa Cruz) were performed as negative control.

siRNA

The 22 nucleotide siRNA duplexes corresponding to nucleotides 191–212 of human Che-1 sequence and to nucleotides 122–143 of the negative control green fluorescent protein (GFP) sequence were synthesized by Xeragon. RNA interference was performed as previously described (Bruno et al., 2002). siRNA-mediated interference experiments of ATM, Chk2, and p65 expression in HCT116 or HFF cells were performed by transfecting SMART pool specific or nonspecific control pool double-stranded RNA oligonucleotides (Dharmacon) using Lipofectamine Plus. For maintenance of G_2 arrest, Che-1 siRNA and GFP siRNA were inserted into pSUPER (Oligoengine).

Supplemental data

Supplemental Data include four figures and Supplemental Experimental Procedures and are available at http://www.cancercell.org/cgi/content/full/10/6/473/DC1/.

Acknowledgments

We thank Drs. V. Sartorelli, M. Levrero, and P.L. Puri for fruitful discussions. We thank Dr. Carlo Del Carlo and Mrs. Rosa Ruscitti for their precious technical assistance. This work was supported by the Italian Association for Cancer Research (AIRC), Telethon project GPO205/01 and GGP05226, Consiglio Nazionale Ricerche (CNR, CU03.00416), and MIUR ex 60%.

Received: December 16, 2005
Revised: July 18, 2006
Accepted: October 5, 2006
Published: December 11, 2006

References

Banin, S., Moyal, L., Shieh, S., Taya, Y., Anderson, C.W., Chessa, L., Smorodinsky, N.I., Prives, C., Reiss, Y., Shiloh, Y., et al. (1998). Enhanced

phosphorylation of p53 by ATM in response to DNA damage. Science *281*, 1674–1677.

Bartek, J., and Lukas, J. (2001). Mammalian G1- and S-phase checkpoints in response to DNA damage. Curr. Opin. Cell Biol. *13*, 738–747.

Bartek, J., and Lukas, J. (2003). Chk1 and Chk2 kinases in checkpoint control and cancer. Cancer Cell *3*, 421–429.

Bartkova, J., Horejsi, Z., Koed, K., Kramer, A., Tort, F., Zieger, K., Guldberg, P., Sehested, M., Nesland, J.M., Lukas, C., et al. (2005). DNA damage response as a candidate anti-cancer barrier in early human tumorigenesis. Nature *434*, 864–870.

Bell, D.W., Varley, J.M., Szydlo, T.E., Kang, D.H., Wahrer, D.C.R., Shannon, K.E., Lubratovich, M., Verselis, S.J., Isselbacher, K.J., Fraumeni, J.F., et al. (1999). Heterozygous germ line hCHK2 mutations in Li-Fraumeni syndrome. Science *286*, 2528–2531.

Boulaire, J., Fotedar, A., and Fotedar, R. (2000). The functions of the cdk-cyclin kinase inhibitor p21WAF1. Pathol. Biol. *48*, 192–202.

Bruno, T., De Angelis, R., De Nicola, F., Barbato, C., Di Padova, M., Corbi, N., Libri, V., Benassi, B., Mattei, E., Chersi, A., et al. (2002). Che-1 affects cell growth by interfering with the recruitment of HDAC1 by Rb. Cancer Cell *2*, 387–399.

Buckbinder, L., Velasco-Miguel, S., Chen, Y., Xu, N., Talbott, R., Gelbert, L., Gao, J., Seizinger, B.R., Gutkind, J.S., and Kley, N. (1997). The p53 tumor suppressor targets a novel regulator of G protein signaling. Proc. Natl. Acad. Sci. USA *94*, 7868–7872.

Bunz, F., Dutriaux, A., Lengauer, C., Waldman, T., Zhou, S., Brown, J.P., Sedivy, J.M., Kinzler, K.W., and Vogelstein, B. (1998). Requirement for p53 and p21 to sustain G2 arrest after DNA damage. Science *28*, 1497–1501.

Burgdorf, S., Leister, P., and Scheidtmann, K.H. (2004). TSG101 interacts with AATF and enhances AR-mediated transcription by promoting its mono-ubiquitination. J. Biol. Chem. *279*, 17524–17534.

Canu, N., Barbato, C., Ciotti, M.T., Serafino, A., Dus, L., and Calissano, P. (2000). Proteasome involvement and accumulation of ubiquinated proteins in cerebellar granule neurons undergoing apoptosis. J. Neurosci. *20*, 589–599.

Delia, D., Mizutani, S., Panigone, S., Tagliabue, E., Fontanella, E., Asada, M., Yamada, T., Taya, Y., Prudente, S., Saviozzi, S., et al. (2000). ATM protein and p53-serine 15 phosphorylation in ataxia-telengiectasia (AT) patients and at heterozygotes. Br. J. Cancer *82*, 1938–1945.

Di Padova, M., Bruno, T., De Nicola, F., Iezzi, S., D'Angelo, C., Gallo, R., Nicosia, D., Corbi, N., Biroccio, A., Floridi, A., et al. (2003). Che-1 arrests human colon carcinoma cell proliferation by displacing HDAC1 from the p21WAF1/CIP1 promoter. J. Biol. Chem. *278*, 36496–36504.

Dunphy, W.G. (1994). The decision to entry in mitosis. Trends Cell Biol. *4*, 202–207.

el-Deiry, W.S., Kern, S.E., Pietenpol, J.A., Kinzler, K.W., and Vogelstein, B. (1992). Definition of a consensus binding site for p53. Nat. Genet. *1*, 45–49.

Fanciulli, M., Bruno, T., Di Padova, M., De Angelis, R., Iezzi, S., Iacobini, C., Floridi, A., and Passananti, C. (2000). Identification of a novel partner of RNA polymerase II subunit *11*, Che-1, which interacts with and affects the growth suppression function of Rb. FASEB J. *14*, 904–912.

Gorgoulis, V.G., Vassiliou, L.-V.F., Karakaidos, P., Zacharatos, P., Kotsinas, A., Liloglou, T., Venere, M., DiTullio, R.A., Jr., Kastrinakis, N.G., Levy, B., et al. (2005). Activation of the DNA damage checkpoint and genomic instability in human precancerous lesions. Nature *434*, 907–913.

Hellin, A.-C., Calmant, P., Gielen, J., Bours, V., and Merville, M.P. (1998). Nuclear factor-κB-dependent regulation of p53 gene expression induced by daunomycin genotoxic drug. Oncogene *16*, 1187–1195.

Hirao, A., Kong, Y.Y., Matsuoka, S., Wakeham, A., Ruland, J., Yoshida, H., Liu, D., Elledge, S.J., and Mak, T.W. (2000). DNA damage-inducible activation of p53 by the checkpoint kinase Chk2. Science *287*, 1824–1827.

Hoeijmakers, J.H. (2001). Genome maintenance mechanisms for preventing cancer. Nature *411*, 366–374.

Huang, S.M., Schonthal, A.H., and Stallcup, M.R. (2001). Enhancement of p53-dependent gene activation by the transcriptional coactivator Zac1. Oncogene *20*, 2134–2143.

Kastan, M.B., and Lim, D. (2000). The many substrates and functions of ATM. Nat. Rev. Mol. Cell Biol. *1*, 179–186.

Khanna, K.K., and Jackson, S.P. (2001). DNA double-strand breaks: signaling, repair and the cancer connection. Nat. Genet. *27*, 247–254.

Kim, S.-T., Lim, D.-S., Canman, C.E., and Kastan, M.B. (1999). Substrate specificities and identification of putative substrates of ATM kinase family members. J. Biol. Chem. *274*, 37538–37543.

Levine, A.J. (1997). p53, the cellular gatekeeper for growth and division. Cell *88*, 323–331.

Lindfors, K., Halttunen, T., Huotari, P., Nupponen, N., Vihinen, M., Visakorpi, T., Maki, M., and Kainulainen, H. (2000). Identification of novel transcription factor-like gene from human intestinal cells. Biochem. Biophys. Res. Commun. *276*, 660–666.

Morla, A.O., Draetta, G., Beach, D., and Wang, J.Y. (1989). Reversible tyrosine phosphorylation of cdc2: dephosphorylation accompanies activation during entry into mitosis. Cell *58*, 193–203.

Muller, H., Bracken, A.P., Vernell, R., Moroni, M.C., Christians, F., Grassilli, E., Prosperini, E., Vigo, E., Oliner, J.D., and Helin, K. (2001). E2Fs regulate the expression of genes involved in differentiation, development, proliferation, and apoptosis. Genes Dev. *15*, 267–285.

O'Neill, T., Dwyer, A.J., Ziv, Y., Chan, D.W., Lees-Miller, S.P., Abraham, R.H., Lai, J.H., Hill, D., Shiloh, Y., Cantley, L.C., et al. (2000). Utilization of oriented peptide libraries to identify substrate motifs selected by ATM. J. Biol. Chem. *275*, 22719–22727.

Okamoto, K., and Beach, D. (1994). Cyclin G is a transcriptional target of the p53 tumor suppressor protein. EMBO J. *13*, 4816–4822.

Okamura, S., Arakawa, H., Tanaka, T., Nakanishi, H., Ng, C.C., Taya, Y., Monden, M., and Nakamura, Y. (2001). p53DINP1, a p53-inducible gene, regulates p53-dependent apoptosis. Mol. Cell *8*, 85–94.

Page, G., Lodige, I., Kogel, D., and Scheidtmann, K.H. (1999). AATF, a novel transcription factor that interacts with Dlk/ZIP kinase and interferes with apoptosis. FEBS Lett. *462*, 187–191.

Pei, X.-H., Nakanishi, Y., Takayama, K., Bai, F., and Hara, N. (1999). Benzo-[a]pyrene activates the human p53 gene through induction of nuclear factor κB activity. J. Biol. Chem. *274*, 35240–35246.

Prives, C., and Hall, P.A. (1999). The p53 pathway. J. Pathol. *187*, 112–126.

Ryan, K.M., Phillips, A.C., and Vousden, K.H. (2001). Regulation and function of the p53 tumor suppressor protein. Curr. Opin. Cell Biol. *13*, 332–337.

Sarkaria, J.N., Busby, E.C., Tibbets, R.S., Roos, P., Taya, Y., Karnitz, L.M., and Abraham, R.T. (1999). Inhibition of ATM and ATR kinase activities by the radiosensitizing agent, caffeine. Cancer Res. *59*, 4375–4382.

Shieh, S.-Y., Ahn, J., Tamai, K., Taya, Y., and Prives, C. (2000). The human homologs of checkpoint kinases Chk1 and Cds1 (Chk2) phosphorylate p53 at multiple DNA damage-inducible sites. Genes Dev. *14*, 289–300.

Shiloh, Y. (2003). ATM and related protein kinases: safeguarding genome integrity. Nat. Rev. Cancer *3*, 155–168.

Stevens, C., Smith, L., and La Thangue, N.B. (2003). Chk2 activates E2F-1 in response to DNA damage. Nat. Cell Biol. *5*, 401–409.

Sun, X., Shimizu, H., and Yamamoto, K.-I. (1995). Identification of a novel p53 promoter element involved in genotoxic stress-inducible p53 gene expression. Mol. Cell. Biol. *8*, 4489–4496.

Takaoka, A., Hayakawa, S., Yanai, H., Stoiber, D., Negishi, H., Kikuchi, H., Sasaki, S., Imai, K., Shibue, T., Honda, K., et al. (2003). Integration of

interferon α/β signaling to p53 responses in tumor suppression and viral defence. Nature *424*, 516–523.

Taylor, W.R., and Stark, G.R. (2001). Regulation of the G2/M transition by p53. Oncogene *20*, 1803–1815.

Thomas, T., Voss, A.K., Petrou, P., and Gruss, P. (2000). The murine gene, *Traube*, is essential for the growth of preimplantation embryos. Dev. Biol. *227*, 324–342.

van Gent, D.C., Hoeijmakers, J.H., and Kanaar, R. (2001). Chromosomal stability and the DNA double-stranded break connection. Nat. Rev. Genet. *2*, 196–206.

Wahl, G.M., and Carr, A.M. (2001). The evolution of diverse biological responses to DNA damage: insights from yeast and p53. Nat. Cell Biol. *3*, 277–286.

Wei, Y., Yu, L., Bowen, J., Gorovsky, M.A., and Allis, C.D. (1999). Phosphorylation of histone H3 is required for proper chromosome condensation and segregation. Cell *97*, 99–109.

Zhou, B.-B.S., and Bartek, J. (2004). Targeting the checkpoint kinases: chemosensitization versus chemoprevention. Nat. Rev. Cancer *4*, 1–10.

Zhou, B.-B.S., and Elledge, S.J. (2000). The DNA damage response: putting check points in perspective. Nature *408*, 433–439.